Graphite Functionalization for Dispersion in a Two-Phase Lubricant Oligomer Mixture

Vinod Kanniah,[1] Binghui Wang,[1] Ying Yang,[2] Eric A. Grulke[1]

[1]*Chemical and Materials Engineering, University of Kentucky, Lexington, Kentucky 40506*
[2]*The Valvoline Company, Lexington, Kentucky, 40509*

Received 5 February 2011; accepted 23 July 2011
DOI 10.1002/app.35574
Published online 17 December 2011 in Wiley Online Library (wileyonlinelibrary.com).

ABSTRACT: Fluids with thermally conductive nanoparticles can provide improved heat transfer. Practical nanofluids will be likely based on lubricating oils for the continuous phase and systems that have extended service temperature ranges. A model system based on poly(α-olefin) synthetic base oil modified with poly(dimethylsiloxane) to lower the mixture's pour point with graphite as a conductive additive was studied. Phase separation of the oligomer mixture occurred at temperatures less than -15°C. Graphite particles were etched using citric acid pretreatment to create hydroxyl and carboxyl groups on their surfaces. A coupling reaction between the hydroxyl groups on graphite and chloro groups on silanes gave rise to poly(α-olefin)-philic graphite particles. Similarly, a coupling reaction between the carboxyl groups on graphite surface and amine groups on silanes gave rise to poly(dimethylsiloxane)-philic graphite particles. SEM, FT-IR, and TG-MS measurements were used to verify the presence of coupling agents on the surface and to estimate the thickness of the coatings. Upon separation of the mixture, each functionalized graphite type migrated exclusively to its preferred phase. © 2011 Wiley Periodicals, Inc. J Appl Polym Sci 125: 165–174, 2012

Key words: dispersions; oligomers; thermogravimetric analysis; hexagonal graphite; functionalization

INTRODUCTION

Nanofillers are inorganic nanoparticles, fibers, nanoclays, carbon-based material, other polymers that have one dimension of 100 nm or less. When nanofillers are added to polymer matrices, the resulting composite may have much different mechanical, optical, electrical, magnetic, and thermal properties than the neat polymer.[1–6] Nanofluids have nanofillers dispersed in a continuous liquid phase and may also have significantly different properties than the neat liquid based on the characteristics of fillers added.[7] When the continuous phase is lubricating oil and the nanofiller are thermally conductive solid, the nanofluid has the potential to improve local heat transfer while reducing friction and providing protection from wear. Nanofluids with improved heat transfer have applications in moving mechanical components in metallurgy, machinery, automotives, railroads, and thermal systems. Nanoparticles, such as multi-walled carbon nanotubes (MWCNT), fullerene, copper oxide, silicon dioxide, and silver, has been used with base fluids (DI water, ethylene glycol, oil, silicon oil, poly-α-olefin) to produce thermally conductive lubricating nanofluids.[8] This introduction addresses practical factors for developing lubricant nanofluids for improved heat transfer, explains the choice of graphite as the particulate additive, and explains how the surface density of functional groups was estimated.

Lubricant nanofluids for improved heat transfer

Developing lubricating nanofluids for improved heat transfer remains a significant challenge. Commercial lubricating oils are complex mixtures of base oils and additives intended to reduce friction and protect metal surfaces from wear and corrosion, transfer heat from critical parts, and suspend particulate impurities, among other things. As the additives are often dissimilar chemically from the base oils, phase separation is a potential issue that needs to be prevented in oil formulation. A recent article on nanofluids for heat transfer has recognized the importance of colloid stability, phase diagrams, and rheology.[9] Should liquid-liquid phase separation occur, it is likely that conventionally dispersed nanoparticles would partition selectively into one phase, reducing the heat transfer properties of the other. Furthermore, there is increasing demand to develop universal base oils that could work over wide temperature ranges.

One approach for developing universal base oils is to combine oligomer lubricants with operating

Correspondence to: E. A. Grulke (egrulke@engr.uky.edu).
Contract grant sponsors: TARDEC.

temperature characteristics that complement each other. This approach was explored using a model system, an oligomer mixture with high thermal conductivity nanoparticles for enhanced heat transfer. Graphite was chosen as filler in a dispersion medium of two-phase mixture: poly(α-olefin) and poly(dimethylsiloxane). Poly(α-olefin) is commonly used in synthetic lubricant composition as a synthetic lubricant base stock.[10] Poly(dimethylsiloxane) oligomers typically have very low viscosities down to their pour points (generally lower than -80°C) and have good shear and thermal stability. A 50 : 50 blend of poly(α-olefin) : poly(dimethylsiloxane) oligomers was chosen for this study as it had lower pour points than the neat poly(α-olefin) oligomer. Phase separation occurs at temperatures less than -15°C. A detailed analysis on the partitioning of this oligomer mixture is reported elsewhere.[11] Oligomer blends of two chemically different materials provide an interesting option for varying lubricant properties for a variety of applications. A critical challenge for such mixtures is controlling their emulsion stability and achieving multiple properties at the same time, thermal conductivity and viscosity in this case.

Graphite particles for thermally conductive dispersions

Graphite particles are dispersed in different medium for commercial applications because of their excellent thermal, electrical, mechanical and magnetic properties. Graphite has good thermal conductivity along its basal planes but much lower thermal conductivity perpendicular to these planes, i.e., across its edges.[12] For high heat transfer coefficients during flow, nanoparticles must be above their percolation limit. In this respect, either disk-like or rod-like particles reach their percolation limits at much lower volume fractions than spherical particles. Uniform dispersions are usually preferred and can be assisted with functional groups on the nanoparticle surfaces. However, high densities of functional groups on the graphite surface can reduce heat transfer by reducing particle-to-particle interactions.

Commercial graphite is chemically inert and comes in varying sizes. Nano-sized graphite particles can be made using different grinding and milling techniques, but graphite's low coefficient of friction makes these processes slow and inefficient. Bead milling of graphite in fluids can be used to achieve dispersions with long-term stability. Graphite dispersion in this work was achieved by creating reactive groups on the carbon surface, followed by either chemical coupling or use of commercial dispersants. Ultrasonication was used to improve particle dispersion. Functionalization alters the surface of the particle and governs particle dispersion, whereas ultrasonication prevents agglomeration and controls particle morphology. Until recently, the only practical functionalization methods reported for graphite involved strong acids or oxidants, similar to the methods used to functionalize carbon nanotubes. Strong acids like H_2SO_4 and strong oxidizing agents like $KMnO_4$ have been used to create high polarity functional groups on carbon materials.[13] These surface oxidation methods are exothermic and also require extensive post-treatment clean-up, including heating, filtration, and washing. Citric acid, a weak organic acid, has been used to create hydroxyl and carboxyl groups on the surface of carbon nanotubes and carbon black.[14,15] It is reportedly used in the functionalization of silica,[16–19] titania,[20–22] and other metal oxide nanoparticles as well. Citric acid treatment does not require complex post treatment. Citric acid has also been used as an acid stabilizer in nanoparticle (alumina, cerium oxide, iron oxide, gold) synthesis.[23–26]

Surface group analysis

The number density of functional groups on the nanoparticle (#/nm^2) is a critical characterization of the actual surface "seen" by the solvent. TG experiments, in which water is a leaving group, have been used to estimate the number density of hydroxyl groups on metal oxide nanoparticles. At elevated temperatures, surface hydroxyl groups will undergo condensation, leaving an oxygen bonded to several metal atoms and generating water. The number of hydroxyl groups per unit mass of nanoparticles is:

$$\#_{OH} = \frac{2(a/18)N}{b} \tag{1}$$

where N is the Avogadro's number, a is the weight loss of water during thermal condensation, and b is the nanoparticle weight. The specific surface area (SSA) of nanodisks (nm^2/g) can be calculated by eq. (2):

$$\mathrm{SSA} = \frac{2\pi(rh + r^2)}{\pi r^2 h\rho} = \frac{2(h + r)}{rh\rho} \tag{2}$$

where r, h, and ρ are the radius, thickness, and density of nanoparticles. The surface density of hydroxyl groups is equal to the ratio of $\#_{OH}$ and SSA.

Thus, the objectives of this work are summarized as:

1. To determine the conditions for controlled etching of graphite (create hydroxyl and carboxyl groups on its surface),
2. To measure the number density of hydroxyl groups before and after functionalization (extent of reaction taking place),

3. To find functionalization pathways to attach coupling agents that enhance the dispersion of graphite nanoparticles in each phase mixture, and
4. To develop functionalized graphite that selectively partition into either poly(a-olefin) or poly(dimethyl siloxane) at phase separation conditions.

The materials described here have not been optimized for specific service conditions, which would be a development effort modifying the morphology of the surface to balance heat transfer and dispersion stability requirements. However, they do provide increased thermal conductivity while ensuring that graphite particles are in each phase if the system should separate under operating conditions.

EXPERIMENTAL

Materials

The oligomer base fluid mixture chosen for this study is poly(dimethylsiloxane) (CAS # 42557-10-8, SK96-10, trimethylsilyl endgroups, GE Silicones, USA) hereafter PDMS and poly(α-olefin) (CAS # 68037-01-4, Chevron Phillips Chemical Company LP, USA) hereafter PAO6. Graphite disks (hexagonal graphite with (002) reflection peak and an interlayer spacing of 0.337 nm)[27] were obtained from GrafTech International. Nano-sized graphite can be used but are not reported here. Analytical grade granular citric acid monohydrate ($C_6H_8O_7 \bullet H_2O$, Formula weight = 210.14) were obtained from Mallinckrodt Chemicals Inc., USA. *N*-octadecyltrichlorosilane (CAS # 112-04-9, molecular weight = 387.93) and amino propyl terminated poly(dimethylsiloxane) (CAS # 106214-84-0, molecular weight = 3000) were obtained from Gelest Inc, USA. Heptane, toluene, and distilled water were analytical grade from Fischer Scientific Inc, USA.

Functionalization

The reaction scheme followed to achieve PAO6-philic and PDMS-philic graphite particles is shown in Figure 1(a) and a detailed description in Figure 1(b). The first step of the functionalization process was generation of hydroxyl and carboxyl groups on the graphite surface; 2 g of citric acid monohydrate was added to 10 ml of distilled water to form an aqueous solution; 100 mg of graphite nanodisks (Sample A) was dispersed into this citric acid solution through ultrasonication at 200 W for 10 min. The dispersion was dried naturally into paste. This paste was heated in the oven at 300°C (decomposition of citric acid takes place around 250°C, Fig. 4) for 30 min. Then it was washed with water (twice) and ethanol

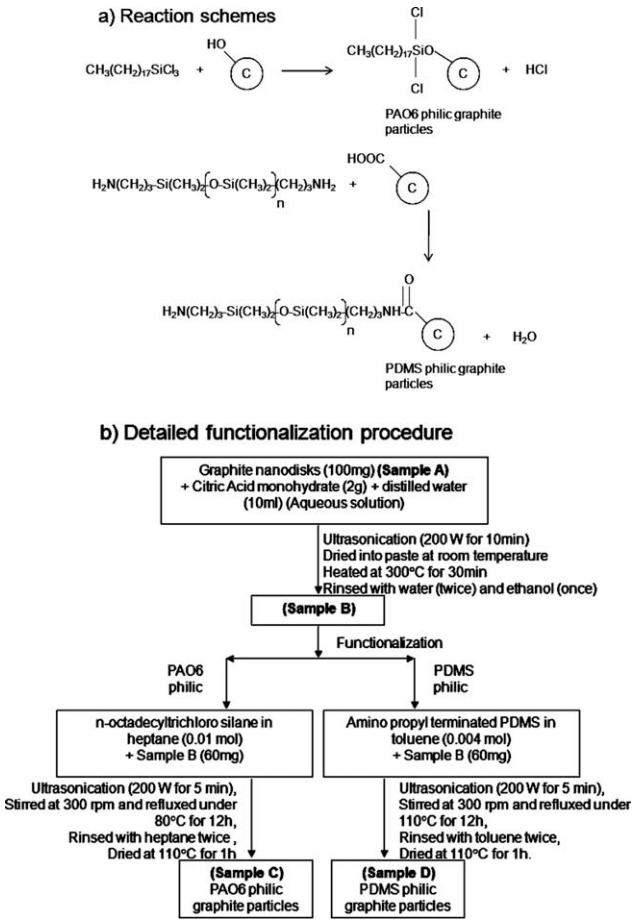

Figure 1 (a) Reaction scheme for PAO6-philic and PDMS-philic graphite particles. (b) Functionalization procedures for PAO6-philic and PDMS-philic graphite particles.

(once) to remove any unreacted citric acid (Sample B). At this temperature, citric acid is liquid and the graphite surface is exposed to a high molar concentration of the oxidizing specie to form a covalent bond through condensation reaction.

Silanes can react directly with the hydroxyl and carboxyl groups created on the nanoparticle surfaces. Hydrogen chloride is a convenient leaving group for this reaction. For synthesizing PAO6-philic graphite, 0.01 mol *n*-octadecyltrichlorosilane was dissolved in heptane; 60 mg of Sample B was added into this beaker and stirred at 300 rpm. The mixture was refluxed at 80°C for 12 h. The product was rinsed with heptane twice to remove the unreacted silanes and dried at 110°C for 1 h to remove the solvents (Sample C). For synthesizing PDMS-philic graphite, amino propyl terminated PDMS with 0.004 mol amine groups were dissolved in toluene; 60 mg of Sample B was added into this beaker and stirred at 300 rpm. The mixture was refluxed under 110°C for 12 h. The product was rinsed with toluene twice to remove the unreacted silanes and dried at 110°C for 1 h to remove the solvents (Sample D).

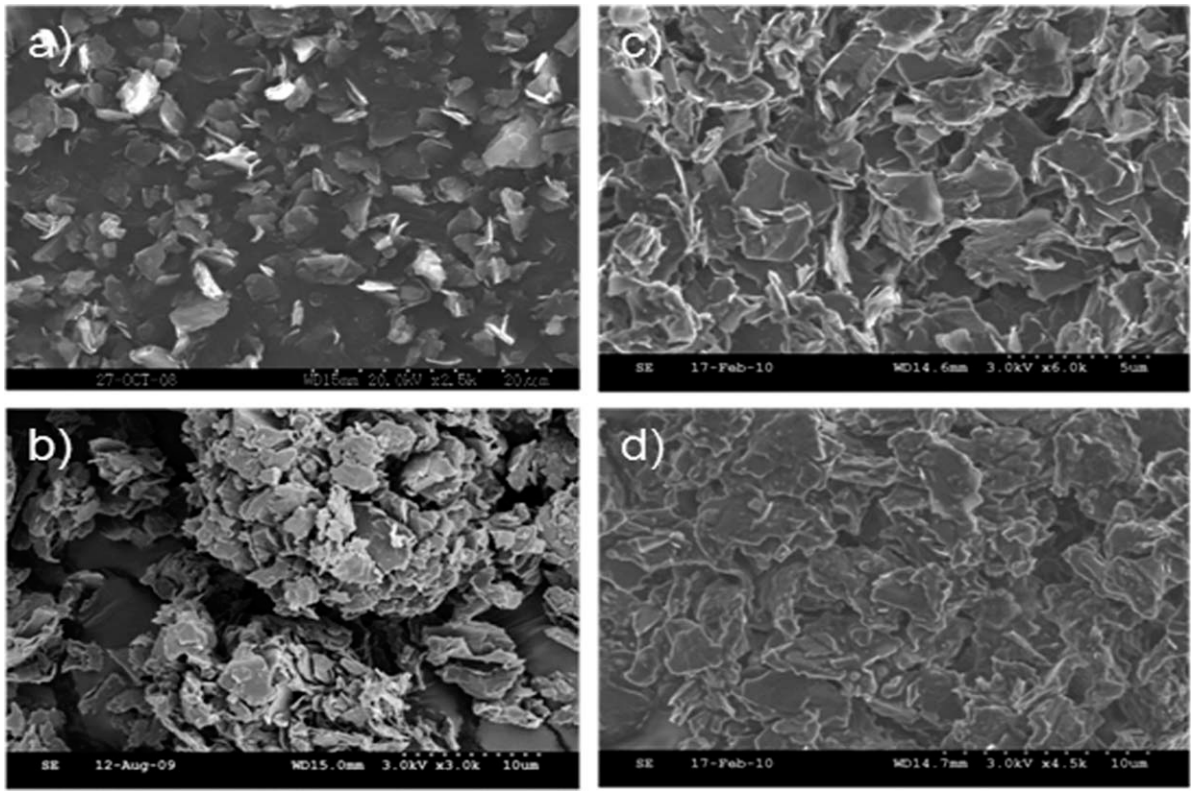

Figure 2 SEM images of (a) as obtained graphite; (b) citric acid treated graphite; (c) PAO6-philic graphite; (d) PDMS-philic graphite.

Characterization

Particle morphology, surface functionality, and dispersion are characterized through scanning electron microscopy (SEM), Fourier transform infrared spectroscopy (FT-IR), thermogravimetric analysis system attached to a mass spectrometer (TG-MS) and partitioning images. Since graphite is nonsperical disk-like particles, it is hard to get accurate particle size distribution information from traditional light scattering devices. Particle morphology of the graphite particles was evaluated using SEM (Model name: Hitachi 3200). The graphite particles were dried at 120°C for 30 min and placed on a conductive carbon tab which was then put over the specimen stub. The samples were blown under dry air for 3 min before being sputter-coated by Au/Pd. A NEXUS 470 FT-IR spectrometer with an ATR accessory suitable for liquid and powder samples was used to identify the types of chemical bonds on a molecule. The window material was ZnSe with a DTGS KBr detector. Potassium bromide (KBr) was used as pellet packing material for powdered samples. Being purely ionic, KBr displays no absorption peaks over the infra-red region. All the graphite samples and KBr were heated in vacuum oven at 120°C for 2 h to remove moisture; 3 mg of graphite particles and 600 mg KBr were mixed; 100 mg of the mixture was pressed to make pellets. The pellets were also then heated at 120°C for 5 min to remove excess moisture if any. The pellets were then scanned through 400–4000 cm^{-1} wavelength range.

TG-MS is used to determine the degradation temperature and number density of hydroxyl groups on the surface of nanoparticles before and after functionalization. TG was operated using a continuous flow of Helium at 100 ml/min metered at standard conditions of 10°C per minute to 100°C, hold 30 min at 100°C, 10°C per minute to 800°C. Empty pan baseline was subtracted from each TG run to eliminate any baseline variation resulting from buoyancy effects. For mass spectrometry, 0–50 amu were scanned using both Faraday and SEM detectors. Partitioning of functionalized graphite was observed by using equal volume two-phase mixtures of PAO6 and PDMS; 10 mg of the functionalized graphite particles were dispersed in 6 ml of the two-phase mixture. The sample was ultrasonicated at 200 W for 3 min and then set inside a refrigerating unit at −18°C for an hour. Images were taken before and after cooling.

RESULTS AND DISCUSSION

Morphology

Figure 2 shows the images so obtained of (a) neat graphite, (b) citric acid treated graphite, (c) PAO6-

philic graphite and (d) PDMS-philic graphite. The neat graphite disks [Fig. 2(a), length scale = 20 μm] had an average diameter and thickness of 2.9 μm and 50 nm, respectively. These disks dispersed uniformly on the conductive carbon tab, suggesting that there were not strong particle-to-particle interactions. The citric acid treated graphite [Fig. 2(b), length scale = 10 μm] showed agglomerates with typical dimensions of ~ 20 μm, about an order of magnitude larger than the individual graphite particles. Since polar groups have been generated on these nanoparticle surfaces, they tend to self-associate rather than interact with the non-polar carbon tab. The PAO6-philic [Fig. 2(c), length scale = 5 μm] and PDMS-philic graphite [Fig. 2(d), length scale = 10 μm] also appear to self-associate but do not form compact agglomerates as did the citric acid treated sample. The two silane coupling agents, one with alkyl chain and the other with an amine-terminated chain with dimethyl siloxane segments, appear to provide coatings that have altered the surface characteristics.

Surface groups—qualitative

Fourier transform infrared spectroscopy (FT-IR) was used to certify the functional groups created through qualitative analysis. FT-IR absorbance spectra of neat PAO6 and neat PDMS oligomers are shown in Figure 3(a). Neat PAO6 oligomer has double peaks at 2840 and 2910 cm^{-1}, corresponding to the stretching vibration of methyl groups (—CH_3) or methylene groups (—CH_2—). The peak at 1450 cm^{-1} corresponds to the bending vibration of —CH_2— and the peak at 720 cm^{-1} corresponds to this group's rocking vibration.[28] Neat PDMS has a sharp peak near 800 cm^{-1} corresponding to asymmetric stretching vibration of Si—CH_3[29] The sharp peak near 1100 cm^{-1} corresponds to symmetrical Si—O—Si stretching,[30] while the narrow peak at 1245 cm^{-1} corresponds to asymmetric C—Si—O stretching.[31] The double peaks at 2890 and 2950 cm^{-1} correspond to the stretching vibration of the methyl groups (—CH_3) attached to each silicon atom in the dimethylsiloxane group.

The spectra of neat graphite, citric acid treated graphite, PAO6-philic graphite, and PDMS-philic graphite is shown in Figure 3(b). Neat graphite has only modest absorbance in this IR range, with no sharp peaks. Citric acid treated graphite showed —OH stretching at ~ 3300 cm^{-1}, which is absent in neat graphite. The peak at 1630 cm^{-1} corresponds to carboxyl groups created by citric acid. PAO6-philic graphite showed a distinct peak at ~ 2850 cm^{-1} that corresponds to —CH_3, —CH_2 stretching. The broad peak from 1050 cm^{-1} to 1300 cm^{-1} corresponds to asymmetric stretching of C—O—Si, generated by the coupling agent's covalent bonds to the graphite surface.[32] The peak near 3400 cm^{-1} corresponds to hydroxyl groups (not associated to absorbed water since the sample preparation took care of it). This was not expected; rather, we anticipated that the chloro groups on the silane would attach to the surface of the nanoparticles.[33] The presence of hydroxyl groups will be discussed as part of the TG-MS results.

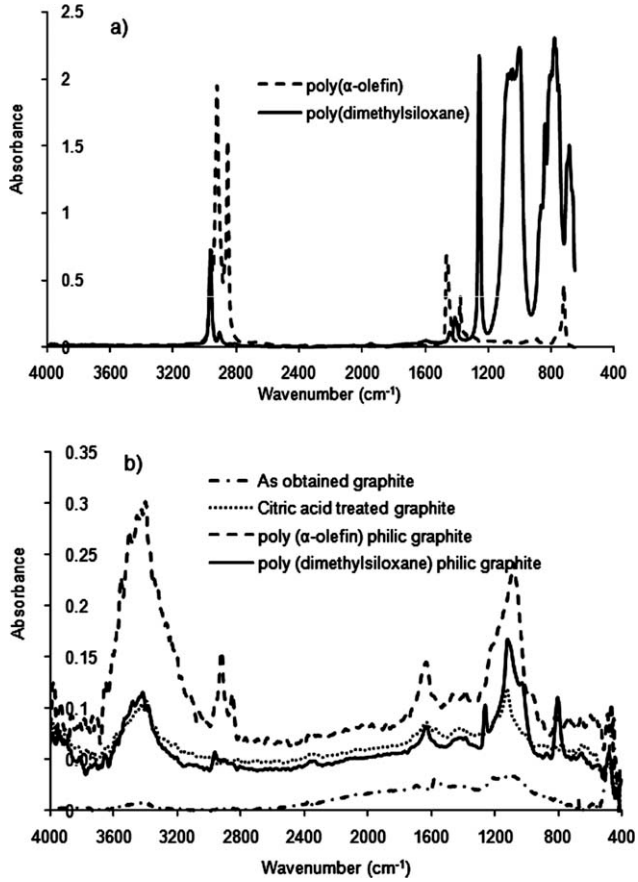

Figure 3 FT-IR absorbance spectra of (a) neat PAO6 and neat PDMS. (PAO6 = dash line; PDMS = solid line). (b) As obtained graphite, citric acid treated graphite, PAO6-philic graphite, and PDMS-philic graphite. (As obtained graphite = dash dot line; citric acid treated graphite = round dot line; PAO6-philic graphite = dash line; PDMS-philic graphite = solid line).

PDMS-philic graphite had a narrow peak at 800 cm^{-1} (asymmetric stretching of Si—CH_3), a sharp peak near 1140 cm^{-1} (symmetrical Si—O—Si), and a narrow peak at 1263 cm^{-1} (asymmetric C—Si—O stretching). These peaks also appear in the FT-IR spectrum of neat PDMS. The peak near 3400 cm^{-1} for hydroxyl groups also appears, as not all surface hydroxyl groups reacted with the coupling agent.

Surface groups—quantitative

The TG-MS data were taken under a helium purge. Under these conditions, the stiochiometry of the decomposition products should closely mirror

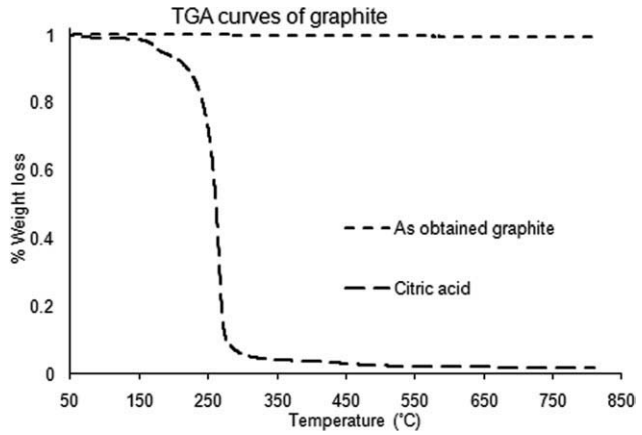

Figure 4 TG curves of as obtained graphite and citric acid. (As obtained graphite = dash line; citric acid = long dash line).

the stiochiometry of the surface groups (citric acid adducts and silane coupling agents). Figure 4 shows TG curves of percent weight loss with temperature for neat graphite and citric acid. Neat graphite did not have any significant weight loss until 800°C because of its high thermal stability. Citric acid melts at ~ 153°C and decomposes before it boils, typically in the range of 250°C. The TG curve for citric acid shows that it is essentially lost at temperatures above 300°C. Evaluation of differential weight loss curves (TG-DTG) and volatile components identified by mass spectroscopy (TG-MS) can lead to quantitative evaluation of surface groups on nanoparticles. Inverse (negative) peaks in the differential weight loss curves show the temperature range over which the weight loss is occurring, while Figures 5–7 show such curves for citric acid treated graphite, PAO6-philic graphite, and PDMS-philic graphite, respectively. Based on TG-MS, a detailed composition of weight loss for (a) neat graphite, (b) citric acid treated graphite, (c) PAO6-philic graphite, and (d) PDMS-philic graphite is reported in Table I.

Neat graphite had a minimal weight loss (0.64%), possibly from dehydration and other decomposition reactions, between 100°C and 750°C. Citric acid treated graphite [Fig. 5(a)] showed several weight loss events. Absorbed water was lost between 50°C and 100°C, with the center of the differential peak at 75°C. The corresponding mass spectrometric peak [Fig. 5(b)] for atomic mass 18 verifies that water was

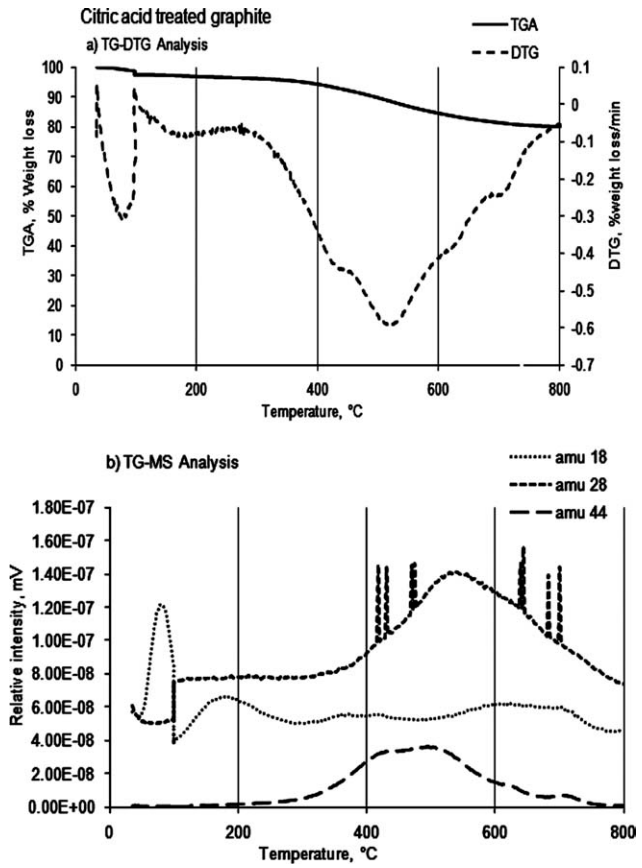

Figure 5 TG-DTG curves and TG-MS curves of citric acid treated graphite. (TG curve = solid line; DTG curve = dash line; amu 18 = round dot line; amu 28 = square dot line; amu 44 = long dash line).

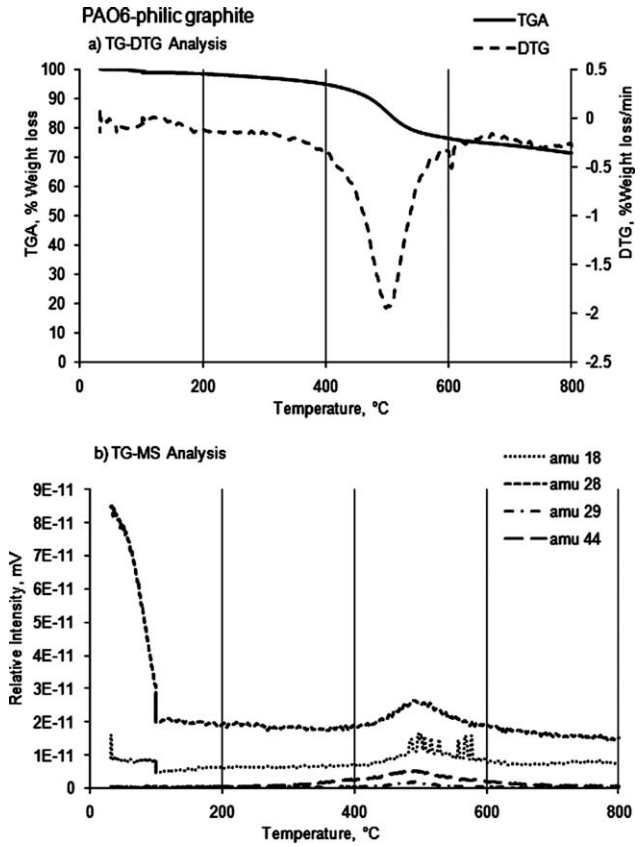

Figure 6 TG- DTG curves and TG-MS curves of PAO6-philic graphite. (TGA curve = solid line; DTG curve = dash line; amu 18 = round dot line; amu 28 = square dot line; amu 29 = dash dot line; amu 44 = long dash line).

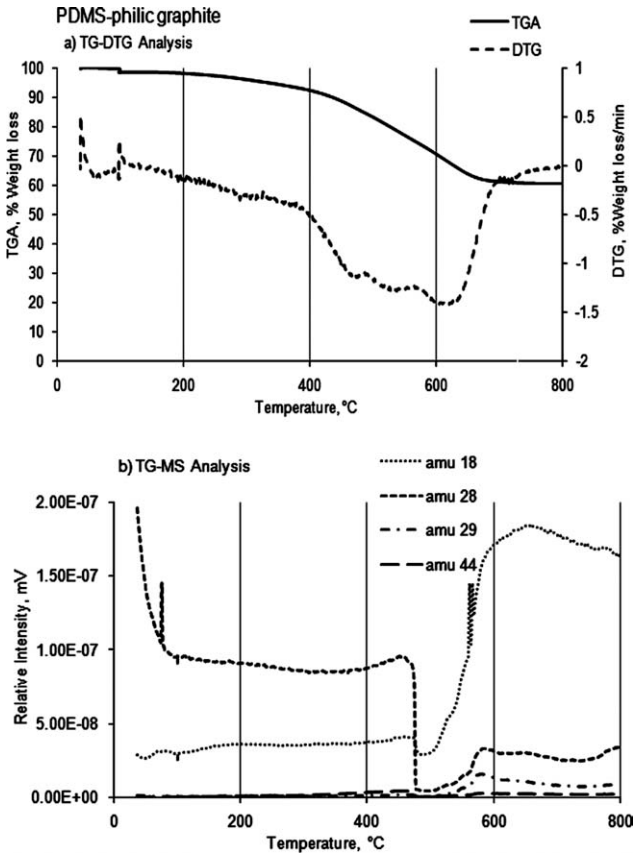

Figure 7 TG-DTG curves and TG-MS curves of PDMS-philic graphite. (TGA curve = solid line; DTG curve = dash line; amu 18 = round dot line; amu 28 = square dot line; amu 29 = dash dot line; amu 44 = long dash line).

lost (2.58% weight loss). Additional water is lost between the range of 100°C and 300°C (1.27% weight loss), which was likely due to dehydration reactions. The major weight loss occurred between 300°C and 750°C, with the center of the peak near 540°C. There are a number of possible decomposition products that would depend on the degradation mechanism. If citric acid followed a pathway that generated itaconic acid (plus water and carbon dioxide as intermediate products), which further decomposed to form more carbon dioxide plus ethylene, the observed products would be:

$$C_6H_8O_7 \xrightarrow{\text{thermal}} C_5H_6O_4 + CO_2 + H_2O$$
$$C_5H_6O_4 \xrightarrow{\text{thermal}} 2CO_2 + 3/2 \cdot H_2C = CH_2$$

This mechanism is consistent with the atomic mass units observed (18 amu (water), 28 amu (ethylene), and 44 amu (carbon dioxide)). The total amount of weight lost to decomposition products was 15.7%. The silane coupling agent for PAO6-philic graphite had a long alkane chain (C_{18}). One possible degradation pathway could involve decomposition to ethylene (C_2H_4, amu 28) and/or ethane radicals ($CH_3CH_2\bullet$, amu 29). If this were the case, then the ratio of ethylene : ethane radicals would be 8 : 1 based on the octadecane chain. Water could be lost as a dehydration product of hydroxyls on the silicon atom of the silane. For PAO6-philic graphite (Fig. 6), the amount of weight loss through desorption of water was 1.27%, less than citric acid treated graphite. This finding is consistent with a functionalization procedure that has created hydrophobic surfaces. However, the amount of water formed by dehydration of hydroxyl groups increased to 1.71%. This was not expected since the silane was expected to couple with surface hydroxyl groups. But other

TABLE I
Composition of Weight Loss Based on TGA-MS. Citric Acid Treated Graphite, Poly(α-olefin)-philic Graphite, and Poly(dimethylsiloxane)-philic Graphite

Temp (°C)	DTG peak (°C)	Reaction	TG-MS peak	% Weight loss
Plain graphite				
100-300		Dehydration		0.27
300-750		Other decomposition		0.37
Citric acid treated graphite				
<100	75	Desorption of water	water (amu 18)	2.58
100–300		Dehydration	water (amu 18)	1.27
300–750	540	Citric acid decomposition	water (amu 18), ethylene (amu 28), CO_2 (amu 44)	15.7
Poly(α-olefin)-philic graphite				
<100	75	Desorption of water	water (amu 18)	1.27
100–300		Dehydration	water (amu 18)	1.71
300–750	520	Decomposition of alkane, citric acid decomposition	ethylene (amu 28), ethane free radical (amu 29), CO_2 (amu 44)	25.6
Poly(dimethylsiloxane)-philic graphite				
<100	50	Desorption of water	water (amu 18)	1.28
100–300		Dehydration, decomposition of CO-NH	water (amu 18), ethylene (amu 28)	2.47
300–750	530; 620	Decomposition of PDMS chains[30,34]; citric acid decomposition	Not evaluated (amu > 50)	35.6

TABLE II
Coating Morphology

Coating	Wt % on NP	Wt % of citric acid, (coating thickness, nm)	Wt % of silane (coating thickness, nm)	Total coating thickness, nm	% Water uptake (from Table I)	Surface density of hydroxyl groups,/ nm^2 (from TGA)	# of monolayers
Citric acid	~ 16 (15.7)	16 (6 nm)	–	6	16.4 (2.58/15.7)	57.4	~ 8 (6/0.72)
PAO6-philic	~ 26 (25.6)	16 (6 nm)	10 (9 nm)	15	5 (1.27/25.6)	87	~ 3 (9/2.62)
PDMS-philic	~ 36 (35.6)	16 (6 nm)	20 (21 nm)	27	3.6 (1.28/35.6)	147	–

researchers using TG to study functionalized titania have also reported higher than expected levels of hydroxyl groups.[33] It should be from the hydrolysis of remained methoxyl groups in the silane attached on the surface of nanoparticles. A significant weight loss of 25.6% was observed at 520°C. This peak with amu 29 corresponds to the formation of ethylene free radical ($CH_3CH_2\bullet$) from the decomposition of alkane chain created.

For PDMS-philic graphite (Fig. 7), the amount of weight loss through desorption of water was 1.28%. This is less than the citric acid treated graphite but the same as PAO6-philic graphite. This means we created hydrophobic surfaces by attaching PDMS chains. There were some dehydration reactions and decomposition of CO—NH at the temperature from 100°C to 300°C which led to 2.47% weight loss. It may arise from the decomposition of amide containing tail of the silane. At 530°C there is a broad peak in DTG and a very sharp decrease of mass (35.6%) in TG-MS associated with the decomposition of PDMS chains. It was the formation of cyclic species form the depolymerization of PDMS.[30,34] TG-MS results shows there was formation of water (amu 18), CO (amu 28), and CO_2 (amu 44). There is a modest trace of ammonia, but no significant peak associated with its detection.

Surface density of hydroxyl groups

Measuring the surface density of hydroxyl groups is important for tailoring functionalization strategies to meet application needs as well as for post-functionalization characterization of the nanoparticle surface. For many applications, the user will want to know what surface groups are available for attachments or chemical interactions as well as the number of such sites per unit area. After functionalization, it is important to know what surface chemistries have been constructed and which surface groups may still be available for interacting with solvents or other molecules in solution. Key steps of this process are identifying which chemical groups are present, determining at what conditions, i.e., temperature, specific groups are degraded, determining what the decomposition products might be, and then relating specific portions of the weight loss curves to these steps.

For citric acid treated graphite, the total weight loss of water by dehydration reaction is from 100°C to 300°C in the TG curve. The total weight loss is 1.27%, which is higher than the weight loss of neat graphite (0.27%). Thus, the surface density of hydroxyl groups on citric acid treated graphite and neat graphite are 57.4/nm^2 and 10/nm^2, respectively. The material balance suggests that about 30% of hydroxyl units on the citric acid have condensed, making this coating lightly crosslinked. This clearly indicates more hydroxyls formed on the surface of graphite nanodisks through citric acid treatment. It is likely that not all of the citric acid carboxyl groups are coupled to the graphite surface. The citric acid coating thickness can be estimated using the weight loss data of Table I and the density of solid citric acid (1.665 g/cm^3) through the simple relation, mass = volume × density. For graphite nanodisks with surface coating, the average original height of graphite disks increases by twice the coating thickness, whereas the average original radius of graphite disks increases by the coating thickness. Using the difference in weight loss accompanied with the difference in volume, the coating thickness is determined by direct calculation assuming a uniform thickness on all disk surfaces for each treatment steps (Table II). The citric acid layer is 15.7 wt % of the functionalized particle weight and has an estimated thickness of 6 nm determined from the mass volume relation. Therefore, it should be difficult to observe in the SEM photomicrograph (Fig. 2). The molecular diameter of citric acid is in the order of ~ 0.7 nm[35]; a shell thickness of 6 nm suggests that about eight monolayers of citric acid are on the particle surface. This estimate is consistent with a partially crosslinked shell of citric acid. The citric acid shell sorbs water at typical lab conditions (~ 16.4 wt %) suggesting that it is fairly hydrophilic.

PAO6-philic graphite released more water of dehydration, ~ 1.7%. The surface density of hydroxyl groups calculated from this weight loss is 87/nm^2 which is more than the surface density of citric acid treated graphite (57.4/nm^2). This was unexpected since the silane molecule should substitute some hydroxy groups on the surface. Rather, they underwent hydrolysis themselves. This phenomenon was observed in the TG analysis of functionalized titania

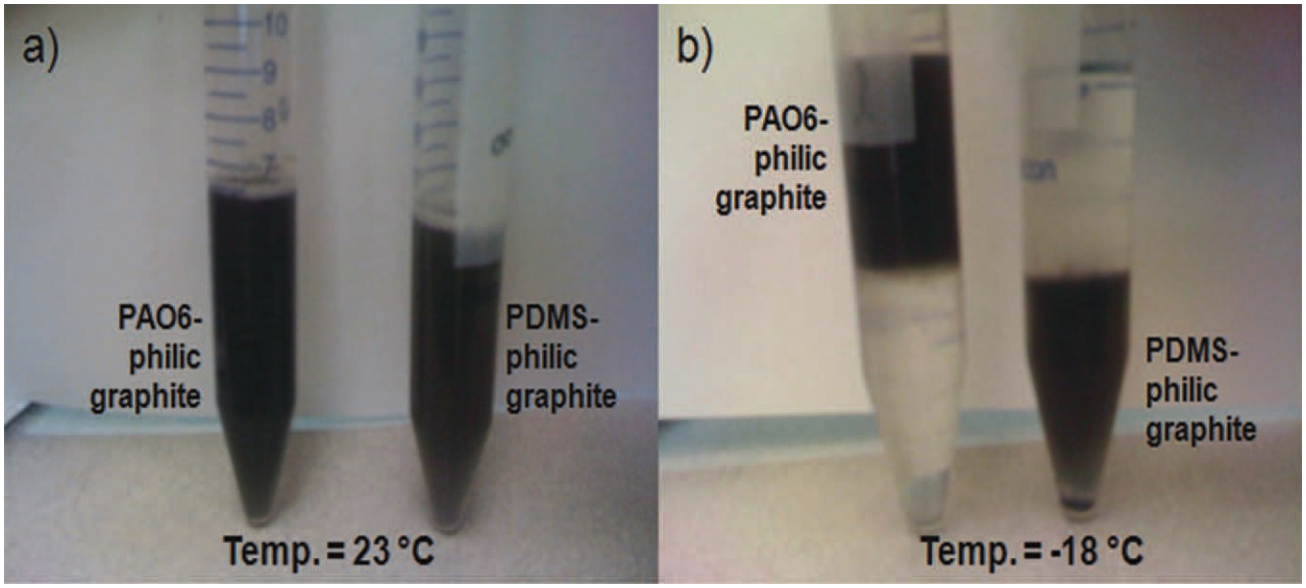

Figure 8 Images of the functionalized particles before and after partitioning in an equal volume PAO6: PDMS oligomer blend. (a) Temp. = 23°C and (b) Temp. = -18°C. Top phase = PAO6 oligomer; bottom phase = PDMS oligomer in each tube. Left tube = PAO6-philic graphite; Right tube = PDMS-philic graphite. [Color figure can be viewed in the online issue, which is available at wileyonlinelibrary.com.]

in literature as well.[33] The coating thickness can be estimated using the method described previously. The citric acid treated graphite with the PAO6-philic silane coating is 25.6 wt % of the functionalized nanoparticle weight. Subtracting the loading of the citric acid, the weight loss of alkane chain is 10% (Table II). If we assume that the Si—$(O)_3$—X group remained on the surface while the alkane part ($CH_3(CH_2)_{17}$, molecular weight = 253) decomposed, then the surface density of alkane chains on the surface is 21/nm^2 [eq. (2)]. Closely packed hydroxyl groups on a flat surface would have a surface density of 10–12 (—OH)/nm^2. If a trifunctional silane group reacted completely, then the surface density of its alkane chains should be $\sim$ 4/nm^2. Since the surface density of hydroxyl groups on the citric acid treated graphite is 57/nm^2, the citric acid coating must be multilayered and contain unreacted hydroxyl groups.

We assume that the silanes react with the outer surface of the citric acid shell. The densities of the citric acid and silane shells are taken to their solid and liquid densities, respectively. Based on these assumptions, the citric acid contributes 6 nm and the PAO6-philic silane contributes an additional 9 nm to the coating (total thickness of 15 nm). However, the silane layer sorbs a much smear fraction of water (5 wt %) than the citric acid layer, suggesting that it is less hydrophilic. Also, the 6 nm thick citric acid surface coating corresponds to 31 citric acid molecules (mass $\times$ N/molecular weight). The theoretical hydroxyl surface density is 124/nm^2 (since four hydroxy groups are present in each citric acid molecule) as opposed to the experimentally (from weight loss) determined hydroxyl surface density of 57.4/nm^2. This suggests that not all hydroxyl groups on the citric acid-treated surface reacted with silanes. The citric acid coating is probably crosslinked with only half of the actual hydroxyls being available for coupling reaction.

For PDMS-philic graphite, the dehydration weight loss occurred over a temperature region (100–300°C) in which the coating was also decomposing. So calculating the surface density of hydroxy groups based on this weight loss gives an overestimate (147/nm^2). Also, above the dehydration temperature, prior work on the degradation of PDMS in the absence of oxygen has shown that multimer siloxanes are formed, with a six member ring being preferred.[30] At a heat rate of 10°C/min, the maximum rate of PDMS decomposition occurred at 611°C,[30] similar to 620°C in this work. The citric acid along with PDMS-philic coating was 36% of the functionalized nanoparticle weight. Unlike PAO6-philic graphite, the decomposition of PDMS chains involves complex mechanism and some compound with Si—O bond may not decompose. It is thus hard to determine the amount of PDMS chains created on the surface. The total coating thickness estimate of 27 nm would include 6 nm attributable to citric acid and 21 nm attributable to the silane. This composite coating absorbed even less water (3.6 wt%) than the PAO6-philic coating. The differences in water sorption by each of these coatings are significant and suggested that sorption of small molecules might be an effective way to investigate the solvency properties of coatings on nanoparticles.

The number of citric acid, octadecyltrichlorosilane, and poly(dimethylsiloxane) molecules per nm^2 over neat graphite are $\sim$ 31, $\sim$ 13, and $\sim$ 4 in their 6 nm, 9 nm, and 21 nm coating over graphite. Citric acid has a corresponding sphere diameter of 0.72 nm[35] and octadecyltrichlorosilane has an extended molecule length of 2.62 nm.[36] Thus, the number of monolayers of citric acid molecules on graphite is $\sim$ 8 (6/0.72) and octadecyltrichlorosilane chains on graphite is 3 (9/2.62) (Table II).

Partitioning of functionalized graphite

Partitioning of functionalized graphite particles before and after partitioning in an equal volume PAO6 : PDMS oligomer blend at (a) Temp. = 23°C and (b) Temp. = -18°C is shown in Figure 8. For both Figure 8(a,b), the left tube has PAO6-philic graphite and the right tube has PDMS-philic graphite particles. At room temperature, the oligomer blend remains miscible as in Figure 8(a). In Figure 8(b) as the temperature is reduced to -18°C: PAO6-philic graphite partitions toward PAO6 in top phase and PDMS-philic graphite partitions toward PDMS in bottom phase. The functionalized nanoparticle disperses uniformly and individually in the PAO6-PDMS blend: there were no agglomerates. This was accomplished by tailoring the silane levels in the coupling reactions to the available hydroxyl groups on the surface. This confirms that the functionalization provides some control over phase separation at low temperatures.

CONCLUSION

Graphite nanoparticles were functionalized to disperse into each phase of a two-phase mixture. A simple and scalable citric acid pretreatment method was used to create hydroxyl and carboxyl groups on graphite surface for functionalization. The etching and silanization processes were not necessarily optimized. The citric acids etch resulted in a 6-nm layer on the graphite surface, greater than a monolayer of this weak acid. Silane levels were tailored to the available hydroxyl groups on the surface, as estimated from TG measurements. Both the PAO6-philic graphite and the PDMS-philic graphite are visible in the blend at room temperature (which is miscible) and partition into the appropriate phase when phase separation occurs at low temperature. All three coatings showed different levels of water absorption, suggesting a method for evaluating the solvency properties of coatings on nanoparticles.

As the authors are not Government employees, this document was only reviewed by OPSEC for export controls, and improper Army association or emblem usage considerations. All other legal considerations are the responsibility of the authors. The authors also thank the Center of Applied Energy Research for TG-MS analysis.

References

1. Alexandre, M.; Dubois, P. Mater Sci Eng R 2000, 28, 1.
2. Ray, S. S.; Okamoto, M. Prog Polym Sci 2003, 28, 1539.
3. Chivrac, F.; Pollet, E.; Averous, L. Mater Sci Eng R 2009, 67, 1.
4. Bredeau, S.; Peeterbroeck, S.; Bonduel, D.; Alexandre, M.; Dubois, P. Polym Int 2008, 57, 547.
5. Fiedler, B.; Gojny, F. H.; Wichmann, M. H. G.; Nolte, M. C. M.; Schulte, K. Compos Sci Technol 2006, 66, 3115.
6. Althues, H.; Henle, J.; Kaskel, S. Chem Soc Rev 2007, 36, 1454.
7. Choi, S. US J Heat Transfer 2009, 131, 0331061.
8. Hwang, Y.; Park, H. S.; Lee, J. K.; Jung, W. H. Curr Appl Phys 2006, 6, e67.
9. Rao, Y. Particuology 2010, 8, 549.
10. Pirro, D. M.; Wessol, A. A. Lubrication Fundamentals; Marcel Dekker: New York, 2001.
11. Kanniah, V.; Forbus, T. R.; Parker, S.; Grulke, E. A. J Appl Polym Sci, 2011, 122, 2915.
12. Garboczi, E. J.; Snyder, K. A.; Douglas, J. F.; Thorpe, M. F. Phys Review E 1995, 52, 819.
13. Titelman, G. I.; Gelman, V.; Bron, S.; Khalfin, R. L.; Cohen, Y.; Bianco-Peled, H. Carbon, 2005, 43, 641.
14. Poh, C. K.; Lim, S. H.; Pan, H.; Lin, J.; Lee, J. Y. J Power Source 2008, 176, 70.
15. Jiang, L.; Gao, L. Carbon 2003, 41, 2923.
16. Sneh, O.; George, S. M. J Phys Chem 1995, 99, 4639.
17. Beck, C.; Hartl, W.; Hempelmann, R. Angew Chem Int Ed 1999, 38, 1297.
18. Shimada, T.; Aoki, K.; Shinoda, Y.; Nakamura, T.; Tokunaga, N.; Inagaki, S.; Hayashi, T. J Am Chem Soc 2003, 125, 4688.
19. Huesing, N.; Schubert, U.; Bernhard, R.; Kiefer, W. Mater Res Soc Symp Proc 1996, 435, 339.
20. Garcia-Gonzalez, C. A.; Fraile, J.; Lopez-Periago, A.; Domingo, C. J Coll Interf Sci 2009, 338, 491.
21. Li, Y.; Yang, F.; Yang, X. Analyst 2009, 134, 2100.
22. Raghuraman, G. K.; Dhamodharan, R. In MACRO International Conference on Polymers for Advanced Technologies, 2004.
23. Masui, T.; Hirai, H.; Imanaka, N.; Adachi, G.; Sakata, T.; Mori, H. J Mater Sci Lett 2002, 21, 489.
24. Kotsmar, C.; Yoon, K. Y.; Yu, H.; Ryoo, Y.; Barth, J.; Shao, S.; Prodanovic, M.; Milner, T. E.; Bryant, S. L.; Huh, C.; Johnston, K. P. Ind Eng Chem Res 2010, 49, 12435.
25. Hidber, P. C.; Graule, T. J.; Gauckler, L. J. J Am Ceram Soc 1996, 79, 1857.
26. Brewer, S. H.; Glomm, W. R.; Johnson, M. C.; Knag, M. K.; Franzen, S. Langmuir 2005, 21, 9303.
27. Shen, T. D.; Ge, W. Q.; Wang, K. Y.; Quan, M. X.; Wang, J. T.; Wei, W. D.; Koch, C. C. Nanostruct Mater 1996, 7, 393.
28. Chercoles, A. R.; San, A. M. M.; Jose Manuel, de la R.; Gomez, M. Anal BioanalChem 2009, 395, 2081.
29. Li, H. Q.; Zeng, X. R.; Deng, H. P. J Appl Polym Sci 2010, 118, 63.
30. Tiwary, A.; Nema, A. K.; Das, C. K.; Nema, S. K. Thermochim Acta 2004, 417, 133.
31. Wright, N.; Hunter, M. J. J Am Chem Soc 1947, 69, 803.
32. Oh, T. Jpn J Appl Phys 12006, 45, 264.
33. Erdem, B.; Hunsicker, R. A.; Simmons, G. W.; Sudol, E. D.; Dimonie, V. L.; El-Aasser, M. S. Langmuir 2001, 17, 2664.
34. Camino, G.; Lokamin, S. M.; Lazzari, M. Polymer 2000, 42, 2395.
35. van Drunen, M. A.; Finsy, R.; Merkus, H. G.; Scarlett, B.; van Rosmalen, G. M. J Cryst Growth 1993, 134, 196.
36. Parikh, A. N.; Schivley, M. A.; Koo, E.; Seshadri, K.; Aurentz, D.; Mueller, K.; Allara, D. L. J Am Chem Soc 1997, 119, 3135.